

Micro objective lens with NA 0.65 for the blue-light small-form-factor optical pickup head

Hsi-Fu Shih,^{1,*} Yuan-Chin Lee,² Yi Chiu,³ David Wei-Chung Chao,⁴
Gung-Ding Lin,¹ Chun-Shin Lu,¹ and Jin-Chern Chiou³

¹Department of Mechanical Engineering, National ChungHsing University,
250 Kuo-Kuang Rd., Taichung, 402 Taiwan, R.O.C.

²Electronics and Optoelectronics Research Labs., Industrial Technology Research Institute,
Chutung, Hsinchu, 310 Taiwan, R.O.C.

³Department of Electric & Control Engineering, National ChiaoTung University,
Hsinchu, 300 Taiwan, R.O.C.

⁴Young Optics Corporation, Science Park, Hsinchu, 300 Taiwan, R.O.C.

*Corresponding author: hfshih@nchu.edu.tw

Abstract: A micro objective lens with the numerical aperture (NA) of 0.65 and clear aperture of 1.1mm was designed, fabricated, and tested for the proposed blue-light small-form-factor optical pickup head system. It adopted the finite optical conjugation and could be produced by using the glass molding technique. The experimental results verify the optical performance near the diffraction-limited focus spot for the applications of high-density portable optical storage systems.

©2008 Optical Society of America

OCIS codes: (220.3630) Lenses; (230.3990) Micro-optical devices; (220.0220) Optical design and fabrication; (210.0210) Optical data storage

References and links

1. B. W. Bell Jr., "DataPlay's mobile recording technology," Tech. Dig. ODS2001, 4-6 (2001).
2. D. L. Blankenbeckler, B. W. Bell, Jr., K. Ramadurai, and R. L. Mahajan, "Recent advancements in Dataplay's small-form-factor optical disc and drive," Jpn. J. Appl. Phys. **45**, 1181-1186 (2006).
3. S. M. Kang, J. E. Lee, W. C. Kim, N. C. Park, Y. P. Park, E. H. Cho, J. S. Sohn, and S. D. Suh, "Development of integrated small-form-factor optical pickup with blu-ray disc specification," Jpn. J. Appl. Phys. **45**, 6723-6729 (2006).
4. H. Nakata, T. Nagata, and H. Tomita, "Ultra compact optical pickup with integrated optical system," Jpn. J. Appl. Phys. **45**, 6713-6717 (2006).
5. J. N. Lee, Hongmin Kim, Y. J. Kim, and S. Kang, "Micro thermal design of swing arm type small form factor optical pick-up system," Microsyst. Tech. **12**, 1093-1097 (2006).
6. M. C. Wu, S. Y. Hsiao, C. Y. Peng, and W. L. Fang, "Development of tracking and focusing micro actuators for dual-stage optical pick-up head," J. Opt. A: Pure Appl. Opt. **8**, S323-S329 (2006).
7. H. D. Cheng, S. Y. Hsiao, M. C. Wu, and W. L. Fang, "Integrated tracking and focusing systems of MEMS optical pickup head," IEEE Trans. Magn. **43**, 805-807 (2007).
8. H. F. Shih, T. P. Yang, M. O. Freeman, J. K. Wang, H. F. Yau, and D. R. Huang, "Holographic laser module with dual wavelength for digital versatile disc optical heads," Jpn. J. Appl. Phys. **38**, 1750-1754 (1999).
9. H. F. Shih, C. L. Chang, K. J. Lee, and C. S. Chang, "Design of optical head with holographic optical element for small form factor drive systems," IEEE Trans. Magn. **41**, 1058-1060 (2005).
10. M. Born, and E. Wolf, *Principles of optics*, 7th ed. (Cambridge University Press 1999), Chap. 9.

1. Introduction

The need of mobility for information technology (IT) products has advanced the development of optical storage drives to be with small form factor (SFF). For achieving the light weight and compact size of an optical pickup head (OPH), microoptical components act the important roles and have been gradually adopted in the SFF optical system [1-7]. Especially, the micro

objective lens is the key component for fulfilling the technology of a SFF OPH. Besides, it is well known that the optical system using a blue laser could effectively increase the storage capacity. Therefore, to develop the blue-light micro objective lens is even more anticipated for the application of blue-light SFF OPH.

Based on the optical system configuration that had been reported for the red-light OPH [8,9], this paper presents a blue-light SFF OPH and a micro objective lens designs that were optimized for the wavelength of 405nm and numerical aperture (NA) of 0.65. By using these designs, the blue-light SFF storage system could be well developed.

2. Objective lens design

The objective lens was first drafted according to the preliminary optical parameters listed in Table 1. We adopted a finite-conjugate relation with the image NA of 0.65 and the laser wavelength of 405nm for the lens. In order to minimize the lens diameter and therefore the OPH dimension, the clear aperture should be as small as possible. After considering the fabrication possibility for the precession glass molding, it was assigned to be 1.1 mm. Since the system is finite-conjugate, the optical magnification of the lens should be fixed. It was planned as the NA of 0.1 for the object side that corresponds to the NA of 0.65 for the focused beam on the disk side. Surface recording with zero cover layer thickness was adopted in the proposed SFF system for effectively reducing the distance between the lens and disk. The lens is a bi-convex type with two even aspheric surfaces. The lens thickness was set to be 0.6 mm and two radiuses were optimized to be 0.63 mm and 3.0 mm, respectively. The K-VC89 from Sumita Inc. was selected as the glass material for the reasons of higher transmittance and larger index of refraction in the blue light range. It could effectively reduce the surface curvatures of the lens and therefore increase the optical and manufacturing tolerance. The material parameters after molding are listed in Table 2. According to the paraxial calculation, the effective focal length of the objective lens was determined to be 670 nm.

Once the first order optics meets the system requirement for a blue-light SFF OPH system, we could further optimize the coefficients of two aspheric surfaces. The optimization conditions need to be followed for preserving the optical parameters stated above. Furthermore, the optimized surfaces should provide the converging capability for focusing the emitting light from the laser to the disk surface inside the smallest spot at both the fields of on-axis and 1° off-axis. Five even aspheric terms are selected for optimization on both surfaces. The surface sag is given as

$$z = \frac{cr^2}{1 + \sqrt{1 - (1+k)c^2r^2}} + \alpha_1 r^2 + \alpha_2 r^4 + \alpha_3 r^6 + \alpha_4 r^8 + \alpha_5 r^{10}, \quad (1)$$

where c is the curvature (the reciprocal of the radius), r is the radial coordinate in lens unit, and k is the conic constant. The optimized coefficients are tabulated in Table 3.

Table 1. Optical Parameters of the SFF OPH

Item	Proposed system
Image-object relation	finite-conjugate system
Disc cover layer thickness	0 mm (surface recording)
Laser wavelength	405 nm
Object NA (laser side)	0.1
Image NA (disk side)	0.65
Focal length	0.670 mm
Clear aperture diameter	1.1 mm

Figure 1(a) shows the simulated optical layout of the lens whereas Fig. 1(b) presents the ray-traced focusing spot on the recording surface of the disk for the on-axis illumination. All

traced rays are concentrated within the Airy disk. Figure 2 shows the root-mean-square (RMS) wavefront error corresponding to the field angle of illumination.

Table 2. Optical parameters of K-VC 89 glass material

Item	Value
Transmittance (10 mm bulk @ 400 nm)	94.3 %
Index of refraction @587.5618 nm (nd)	1.8054
Abbe number (Vd)	41.64
Transformation point (Tg)	528 °C
Yielding point (At)	559 °C

Table 3. Coefficients of the surface sag of two aspheric surfaces

Item	Surface 1 (S1)	Surface 2 (S2)
Radius	0.6285543	-3
Conic	-0.725968	-5.514276
α_1	0	0
α_2	0.048940086	0.78716313
α_3	-0.54656561	-6.870713
α_4	1.2654383	17.112211
α_5	-9.7401643	-18.21906

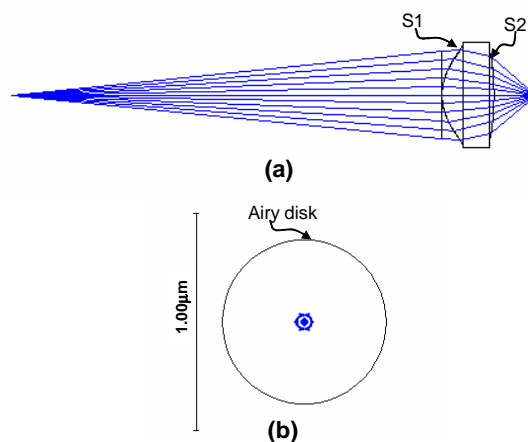


Fig. 1. Simulations of the objective lens for (a) the optical layout and (b) the focusing spot.

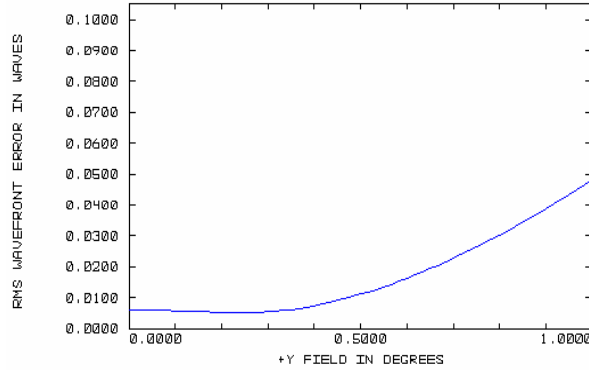


Fig. 2. RMS wavefront error vs field.

3. Design of the SFF optical pickup head

With this objective lens, the optical system of the proposed blue-light SFF OPH was arranged. Figure 3(a) shows the schematic diagram of the OPH and Fig. 3(b) describes the relative placement of all components on the substrate. An edge-emitting laser chip is bonded on a silicon substrate with a 45° etching micromirror. It reflects the laser beam upward to a 45° microprism MP1, which is upside-down bonded on the substrate. After reflected by MP1, the beam is redirected by the other 45° prism MP2 to vertically enter the holographic optical element (HOE). The zeroth-order light that passes through the HOE is focused on the disk by the objective lens. On the returning path, the beam is diffracted by the HOE, reflected by the MP1 and MP2, and finally projected onto the photodetector (PD). The MP1 and MP2 act as not only reflectors but also two spacers for supporting the HOE and objective lens. The astigmatic detection is used for generating the focusing error signal (FES) from the HOE diffraction. The HOE pattern could be designed by the binary optics technology and has the wavefront represented by

$$\phi(x, y) = \sum_{m=0}^M \sum_{n=0}^N C_{mn} x^m y^n. \quad (2)$$

In this design, we took six terms of the phase polynomial as

$$\phi(x, y) = C_{01}y + C_{20}x^2 + C_{11}xy + C_{02}y^2 + C_{21}x^2y + C_{03}y^3, \quad (3)$$

where the $C_{01}y$ provides the diffraction angle in the y -direction, the $C_{20}x^2$, $C_{11}xy$, $C_{02}y^2$ serve as the combination of a focusing lens and a cylindrical lens that converges the beam and generates the astigmatism, and the remaining terms are used for correcting the coma, spherical and high order aberrations. Figure 4(a) presents the optical modeling of the OPH system and Fig. 4(b) gives the simulation result for the FES (so-called S-curve), which is in a symmetric shape. The optimized coefficients of the phase polynomial of the HOE surface are listed in Table 4. Using these coefficients, the binary diffractive pattern of the HOE can be accordingly designed.

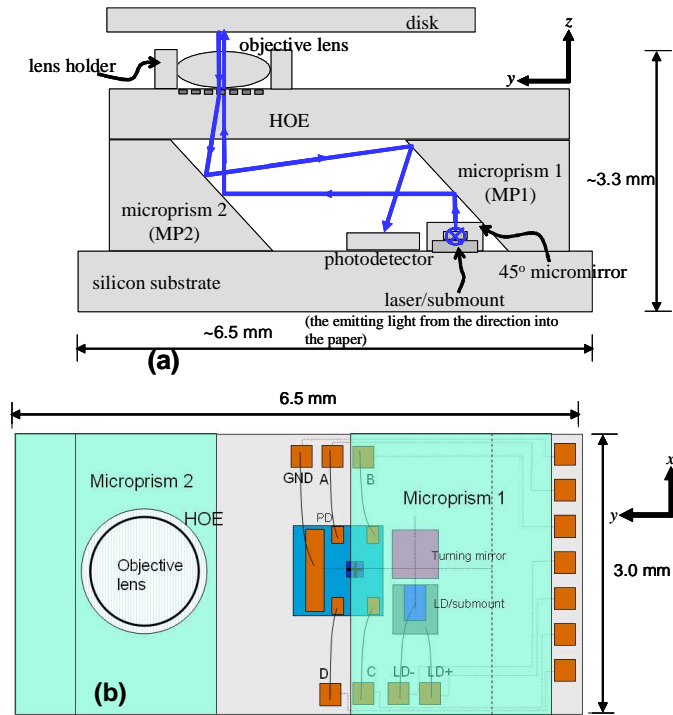


Fig. 3. (a) Schematic diagram of the blue-light SFF OPH and (b) relative placement of all components on the substrate.

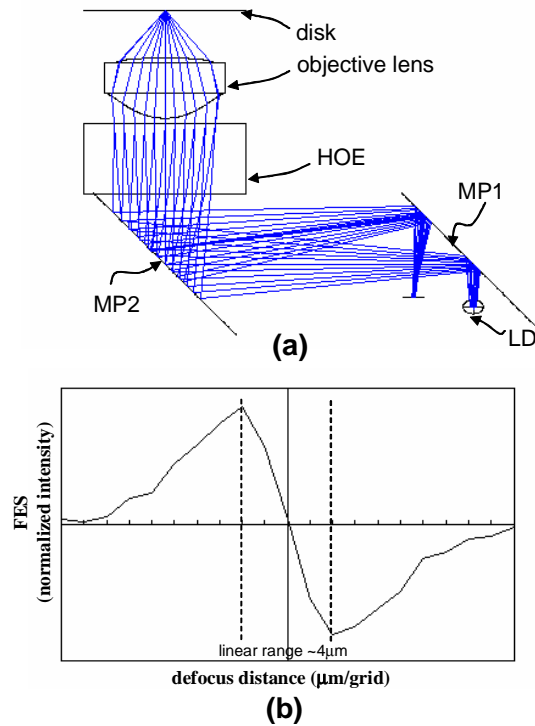


Fig. 4. (a) Optical modeling of the blue-light SFF OPH system and (b) the simulated S-curve for the FES.

Table 4. Coefficients of the phase polynomial of the HOE surface^a

Coefficient	C_{01}	C_{20}	C_{11}	C_{02}	C_{21}	C_{03}
Value	-2007	118.841699	129.261428	93.450824	41.47631	40.841915

^aThe unit of x and y of the phase polynomial is in mm.

4. Fabrication of the micro objective lens

The surface curvature of the finite-conjugate objective lens with NA 0.65 is steeper than that of the infinite-conjugate objective lens with the same NA. Besides using the glass material of higher index of refraction, advanced and precision diamond turning machine was applied to produce the mold insert with sharp surface shapes. After the turning, the heavy metal alloy was coated on the mold insert surface as the hard coating. The produced mold inserts of two lens surfaces and the outer mold are shown in Fig. 5. With these molds, continuous glass molding process with single mold was adopted to fabricate the objective lens. Figure 6 shows the pictures from top and side views of the fabricated lens.

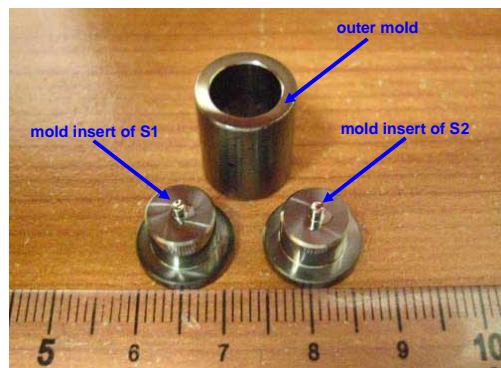


Fig. 5. Picture of the mold inserts of two lens surfaces and the outer mold.

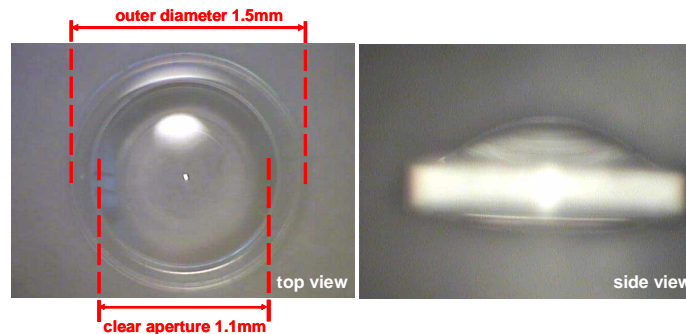


Fig. 6. Pictures of the fabricated lens from the top and side views.

5. Experimental results

In order to verify the optical performance of the fabricated lens, the precision profile meter was first applied to measure the surface form shapes. Figure 7 shows the measured results for both lens surfaces from a typical fabricated sample. The tested data are summarized on Table 5. Because the S1 surface has a sharper curvature, it gets the higher form deviation than that of S2 surface. The total root-mean-square (RMS) form deviation is 30.6 nm. It is near the Maréchal criterion of one fourteenth wavelength of 405 nm, which is 28.93 nm, for achieving the diffraction-limited focusing capability [10]. For further verification, the spot checker was adopted to measure the focusing spot size by using the illumination of a 405 nm blue laser under the same image-object conjugation as described. Figure 8 shows the practical focus spot distribution and intensity profiles from radial and tangential directions. It gives the measured

spot size of $0.356 \mu\text{m}$ and $0.347 \mu\text{m}$ in the tangential and radial directions, respectively. According to Eq. (4), the theoretical full-width-half-maximum (FWHM) spot size D_{sp} is $0.324 \mu\text{m}$ for both directions. Although the measured spot size is bigger than the theoretical value by around 10% and 7% in the tangential and radial directions, respectively, it still stays within the acceptable range when the disc specification of data pits is the same as that of the HD-DVD.

$$D_{sp} = 0.52 \frac{\lambda}{NA} \quad (4)$$

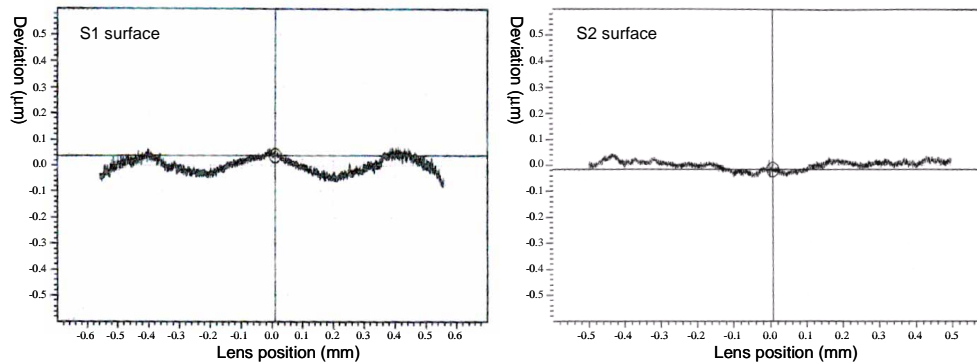


Fig. 7. Form deviation measurement of both surfaces of a fabricated lens.

Table 5. Tested surface data of a fabricated lens.

Item	Surface 1 (S1)	Surface 2 (S2)
Figure (nm)	28.6340	-14.5867
RMS (nm)	25.7197	16.5779
Ra (nm)	21.4001	13.2570
Rt (nm)	155.3	92.2413

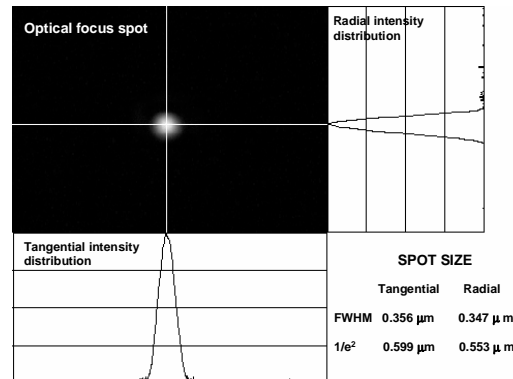


Fig. 8. Optical focus spot distribution and intensity profile measurement.

6. Discussion and conclusion

We have presented a blue-light SFF OPH configuration combined with a finite-conjugate micro objective lens design. Simulation and experimental results are satisfactory and provide the feasibility of realizing the high-density storage system in compactness. The prototype of the objective lens was fabricated by the technique of glass molding and tested to have the

optical quality near the diffraction-limited focusing capability. Nevertheless, in order to reach the perfect diffraction-limited lens quality, precision for mold insert and molding process are still needed to be improved. Currently, we are proceeding to produce the other components of the OPH system. Based on the design and experiments in this paper, a blue-light SFF OPH will be possibly implemented in the near future.

Acknowledgments

The authors would like to acknowledge Mr. Rong-Jyh Chang for his help on the machining of testing jigs. They also thank the Ministry of Economic Affairs and the National Science Council of Taiwan. This work was supported in part by the MOEA under grant 96-EC-17-A-07-S1-011 and by NSC under grant NSC 96-2221-E-005-058-MY3.